

# Interplay of causticity and vorticality within the complex quantum Hamilton-Jacobi formalism

A. S. Sanz\* and S. Miret-Artés†

*Instituto de Física Fundamental “Blas Cabrera”,*

*Consejo Superior de Investigaciones Científicas, Serrano 123, 28006 Madrid, Spain*

(Dated: April 20, 2019)

The dynamics associated with interference processes is analyzed in the light of the complex quantum Hamilton-Jacobi formalism, and using as a working model the collinear collision of two Gaussian wave packets. As shown, the interference fringes appearing during the scattering process lead to the appearance of quantum vortices in the complex plane, which break off the causticity associated with the free propagation of each wave packet. Moreover, an unambiguous connection between the complex quantum trajectories and their real counterparts is established.

PACS numbers: 03.65.Ta, 03.65.Ca

Nowadays, the detailed study of the dynamical evolution of quantum systems with a relative large number of degrees of freedom is an important and challenging issue. Realistic simulations of many phenomena of interest result prohibitive computationally via the time-dependent Schrödinger equation. Aimed to avoid this computational inconvenience, different trajectory-based approaches are currently being developed [1]. One of these approaches is based on the quantum Hamilton-Jacobi formalism [2, 3, 4, 5]: after considering the transformation relation  $\Psi(x, t) = e^{i\bar{S}(x, t)/\hbar}$ , the time-dependent Schrödinger equation for a particle of mass  $m$  transforms into a complex quantum Hamilton-Jacobi equation,

$$\frac{\partial \bar{S}}{\partial t} + \frac{(\nabla \bar{S})^2}{2m} + V_{\text{eff}} = 0. \quad (1)$$

Here,  $V_{\text{eff}} \equiv V - (i\hbar/2m)\nabla^2 \bar{S}$  is an effective potential whose second term on the r.h.s. is a *nonlocal* complex quantum potential. From the standard Hamilton-Jacobi theory, one can assume the existence of a family of characteristics or trajectories satisfying the motion law (or “guidance” condition)

$$\dot{z} = \frac{\nabla \bar{S}}{m} = \frac{\hbar}{im} \frac{\nabla \bar{\Psi}}{\bar{\Psi}}. \quad (2)$$

Note that, since this complex velocity field depends on  $\bar{S}$ ,  $z$  has to be necessarily a complex variable. Because of analytic continuation, both  $\bar{S}$  and  $\bar{\Psi} \equiv \Psi(z, t)$  will then be complex functions. This approach has been shown to be relatively stable and efficient computationally for low-dimensional systems [6, 7, 8].

At a theoretical level, the complex quantum Hamilton-Jacobi approach has been basically used to study the motional regimes associated with different systems described by time-independent wave functions [4, 9]; little attention has been paid to time-dependent problems [10], in particular, to quantum interference, which is central in many actual and important research fields (e.g., quantum control and quantum information and computation).

Taking into account the increasing interest in the complex quantum Hamilton-Jacobi formalism as a computational tool, in this Letter we provide a novel analysis of quantum interference in the light of this formalism, where the quantum dynamics is unfolded to the complex plane. This unfolding gives rise to unexpected and surprising features even for low-dimensional systems. In particular, we show how quantum vorticality appears in one-dimensional processes, such as the collinear collision of two Gaussian wave packets, despite two dimensions are needed at least in order to observe it within a real quantum Hamilton-Jacobi approach [11]. Though apparently simple, this is a very general problem whose analysis is aimed to provide the basis to understand the physics underlying more complicated interference processes. The vortical dynamics observed in the complex plane is a natural consequence of the formation of a fringe pattern in the real configuration space, and gives rise to a very rich and complex topology in the different quantum fields involved. Moreover, it breaks off the regularity of the caustics observed in free propagating wave packets [12].

The problem of the collinear collision of two identical Gaussian wave packets can be described analytically by the (time-dependent) wave function

$$\Psi(x, t) = \mathcal{N} [\psi_1(x, t) + \psi_2(x, t)], \quad (3)$$

where

$$\psi_j(x, t) = \left( \frac{1}{2\pi\bar{\sigma}_t^2} \right)^{1/4} e^{-(x-a_j-v_0^{(j)}t)^2/4\bar{\sigma}_t\sigma_0 + ip_0^{(j)}x/\hbar - iEt/\hbar}, \quad (4)$$

with  $j = 1, 2$  and  $\mathcal{N}$  being the normalizing factor. In Eq. (4),  $\bar{\sigma}_t = \sigma_0(1 + i\hbar t/2m\sigma_0^2)$  is the complex time-dependent spreading and  $\sigma_t = \sigma_0[1 + (\hbar t/2m\sigma_0^2)^2]^{1/2}$  is the actual (real) spreading of the Gaussian wave packet. On the other hand,  $\sigma_0$  is the initial width,  $a_j$  is the initial position, and  $v_0^{(j)} = p_0^{(j)}/m$  and  $E = p_0^2/2m$  are the velocity and energy associated with the free propagation of a particle with mass  $m$ , respectively. The dynamical evolution of the wave packet (4) is characterized by two

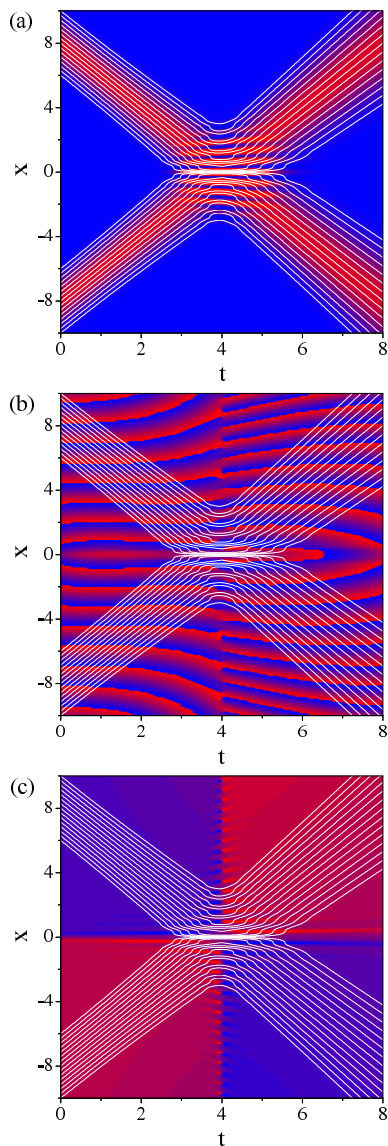


FIG. 1: Space-time contour plots of the probability density (a), phase (b) and velocity field (c). The associate flux lines or trajectories have been represented in all plots to make easier their understanding. The initial values are  $\sigma_0 = 1$ ,  $a_j = \mp 8$ , and  $v_0^{(j)} = \pm 2$  (with  $j = 1, 2$ ), for a particle with unit mass (arbitrary units are used). The color scale from red to blue ranges from high values of the corresponding field to the lower ones [0 in (a); negative in (b) and (c)].

types of effects [13]: translation and spreading. The former can be regarded as a classical effect, while the latter is of quantum origin.

The dynamical evolution of (3) is relatively simple in the real space; the associate probability density, phase, and velocity field have been plotted as a function of time in the three panels of Fig. 1 [(a), (b) and (c), respectively]. Several flux lines or trajectories associated with this problem (white solid lines) have also been displayed in the three panels; these trajectories are solutions of

a real quantum Hamilton-Jacobi equation. As seen in Fig. 1(a), the interference of the two wave packets leads to the appearance of a nodal structure in the probability density, which make the trajectories avoid certain space regions. These nodes strongly affect the space-time structures of both the phase of the wave function [see Fig. 1(b)] and the associate velocity field [see Fig. 1(c)]. Sudden “jumps” in the phase, from  $-\pi$  (blue) to  $\pi$  (red), are observed near  $t = 4$ , the time of maximal interference. This provokes that the velocity field undergoes (also around  $t = 4$ ) a sharp variation from positive to negative values (and vice versa). Note that this field divides the configuration space basically into two well-defined dynamical regions: in one region the momentum is positive (reddish regions), while in the other one it is negative (blueish). Separating these regions there is a sort of interphase acting like a (fictitious) barrier. As time evolves, a series of nodes starts appearing. Then, at  $t = 4$ , the dynamics are reversed and the trajectories change their direction.

Around  $x = 0$  the velocity field displays some local periodic maxima (in the positive momentum region) and minima (in the negative momentum region), which become more important as time evolves, and that, after the maximal interference, they exchange their topology (maxima become minima and vice versa). These structures are strongly connected with the formation of the nodal structure: they arise from the initial overlapping of both wave packets, which have opposite propagation velocities. Only when both wave packets are very far apart (e.g., after the collision), this effect disappears. Thus, note that, regardless the value of the probability density [and provided  $\rho(x, t) \neq 0$ ], the dynamics are always well defined at any space point and time. As seen below, this has a very nice counterpart within the complex description of this scattering process.

In the complex version of the wave packet interference process, the dynamics becomes richer. This one-dimensional problem transforms into a two-dimensional one, thus the dynamics exhibiting more complicated features when represented in an Argand plot. In Fig. 2 several snapshots of the complex probability density and velocity field (the latter expressed separately as its modulus and phase) are plotted to show their dynamical evolution. Several remarks are worth stressing. First, the real (time-dependent) wave function,  $\Psi(x, t)$ , corresponds to the crossing of the complex wave function,  $\Psi(z, t)$ , with the real axis at each time, as can be seen in the upper row of Fig. 2. Second,  $\Psi(z, t)$  satisfies the normalization condition *only* along the real axis, but not in general in the complex plane. And, third, as can be seen in the progression shown in Fig. 2, the time-evolution of the complex wave function is similar to the effect of having compressed a watch spring: once the spring is left free, it spreads in a sort of rotational motion. It is interesting to note that at the very moment of maximum interference ( $t = 4$ ), the nodal structure (a set of aligned nodes) just

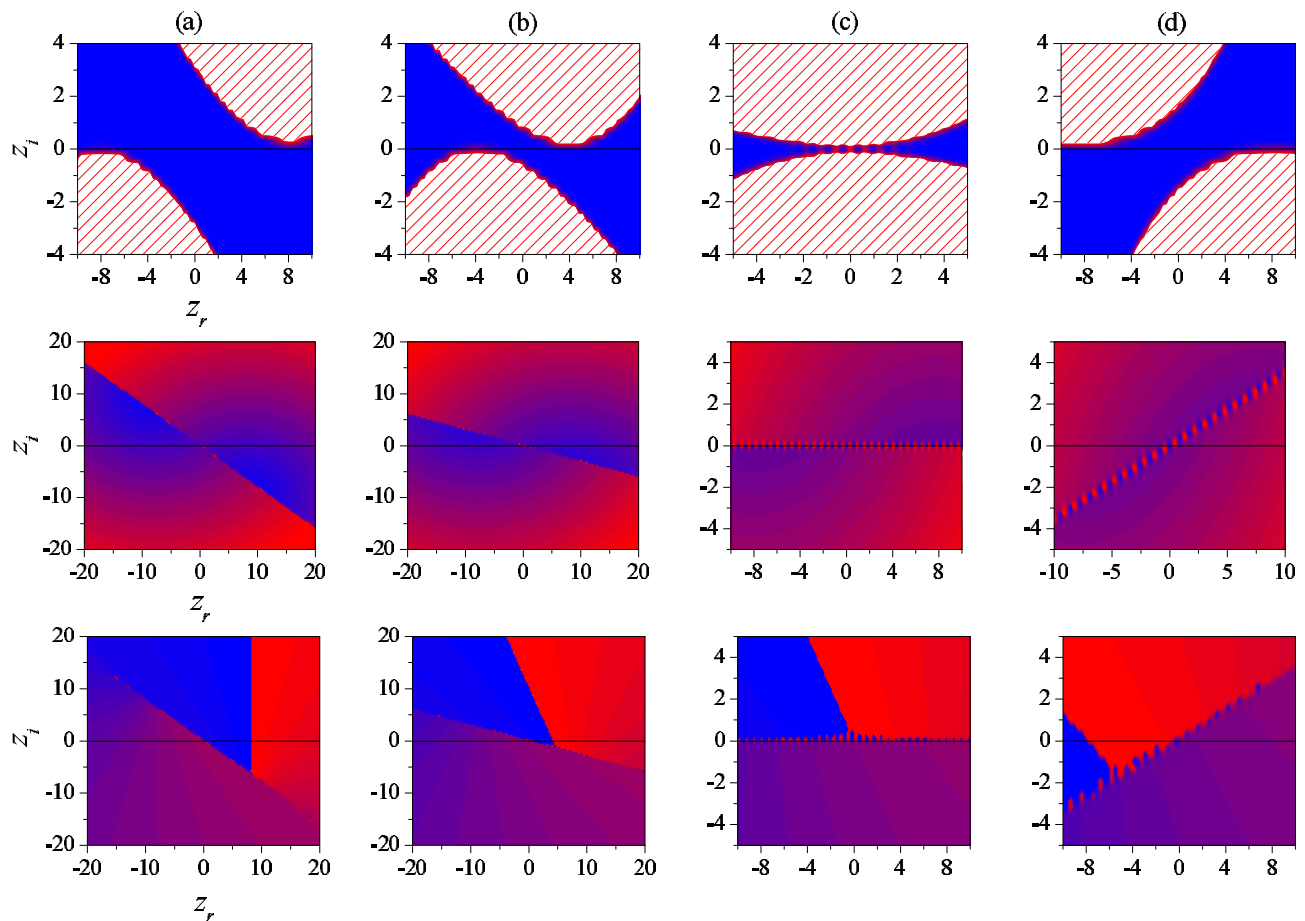


FIG. 2: Contour plots showing the dynamical evolution of the complex wave function,  $\bar{\Psi}$ , in the complex plane and the associate (complex) velocity field at: (a)  $t = 0$ , (b)  $t = 2$ , (c)  $t = 4$ , and (d)  $t = 8$  (arbitrary units are used). The three rows, from top to bottom, correspond to the complex probability density, and the modulus and phase of the complex velocity field.

sits on the real axis. After that, the nodal alignment still remains but it is out of the real axis. This means that the interference observed in the real configuration space decreases [and even disappears; observe in the upper panel of Fig. 2(d) that at  $t = 8$  we get again two separate wave packets] although it remains on the complex plane.

In Fig. 3 different families of complex trajectories (or flux lines) crossing the real axis at the same four times considered in Fig. 2 are plotted. As can be clearly seen, in principle there is no any dynamical relationship between real and complex trajectories. However, a sort of “static” relationship can be established, which is similar to the relation existing between the real and complex wave functions: the position of a particle following a real trajectories at a given time is the crossing of a certain complex trajectory with the real axis at that time. Therefore, the position of the particle along the real trajectory corresponds to the crossings of *different* complex trajectories with the real axis (one crossing for each position at each time). This property allows to define a real trajectory as a family of complex trajectories such that their subsequent crossings (in time) with the real axis gener-

ate that real trajectory. This explains why, at a given time, one needs to consider *isochrones* when using computational methods based on complex trajectories, i.e., families of complex trajectories reaching the real axis at a given time  $t$  (every isochrone is thus associated with a different real trajectory).

In Fig. 3(c), we can see a family of isochrones displaying vortical dynamics. This is in contrast with the analog situation in real configuration space, where vortical motion can only be observed for two (or higher) dimensional problems [11]. The presence of (complex) vortices can be explained as their appearance in the real configuration space. Under certain conditions, as in classical fluids, vortices can appear in the quantum flow evolution. These conditions are linked to the complex character of  $\bar{\Psi}$ : except for a constant in its phase,  $\bar{\Psi}$  is uniquely determined, i.e., it remains invariant under a change of phase if the condition

$$\bar{S}'(z, t) = \bar{S}(z, t) + 2n\pi\hbar \quad (5)$$

is satisfied, with  $n$  being an integer number. Since  $\bar{\Psi}$  is a smooth function, discontinuities in its phase ( $n \neq 0$ )

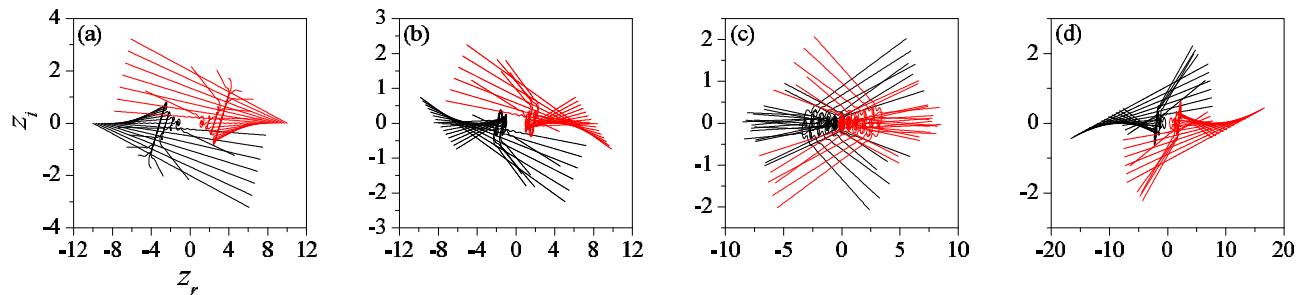


FIG. 3: Isochrones crossing the real axis ( $z_i = 0$ ) at: (a)  $t = 0$ , (b)  $t = 2$ , (c)  $t = 4$ , and (d)  $t = 8$ , in accordance with the snapshots shown in Fig. 2 (arbitrary units are used). All the trajectories are propagated (from  $t = 0$ ) up to  $t = 8$ ; the crossing points correspond to the same positions reached by the real trajectories in Fig. 1 at the corresponding times. Black and red trajectories are associated with  $\psi_1$  and  $\psi_2$ , respectively.

can only occur in nodal regions where the wave function vanishes and the phase displays “jumps” because its multivaluedness. These discontinuities give rise to a vortical dynamics as can be inferred from the circulation of the phase  $\bar{S}$  along a closed path. When  $n \neq 0$ , the velocity field is rotational leading to the formation of quantum vortices around nodal regions.

Another very important aspect of this dynamics is the presence of caustics, which can be clearly observed in panels (a), (b) and (d) of Fig. 3. Before and after the maximum interaction takes place, the *caustics* observed in the free propagation of wave packets in the complex plane [12] can be observed because of the nearly free motion of  $\psi_1$  and  $\psi_2$ . However, they get broken because of the development of the vortical dynamics, which prevents the isochrones in Fig. 3(c) to display the corresponding caustics.

Summarizing, quantum trajectory based methods are proven to be a valuable numerical tool to explore high-dimensional problems in quantum mechanics. As in other parts of Physics, generalizing to the complex plane yields numerical simplifications of the problems of interest. However, from a theoretical and interpretive viewpoint, we have shown that even in the case of very simple processes (with a simple dynamics in the real configuration space), such as the frontal collision of two Gaussian wave packets, very complicated dynamics and topologies can appear, which deserve much consideration in order to understand more complicated problems. Because of the two-dimensionality introduced by the complex treatment in simple one-dimensional problems, vorticality and causticity might lead to important physical phenomena (e.g., *complex quantum chaos*). In this sense, a next natural step in this kind of studies, which is currently being developed, is their extension to phenomena where both interference and diffraction play a fundamental role, such as the Talbot effect [14].

This work has been supported by DGICYT (Spain) un-

der project with reference FIS2004-02461. A.S. Sanz acknowledges the Spanish Ministry of Education and Science for a “Juan de la Cierva” Contract.

---

\* Electronic address: asanz@imaff.cfmac.csic.es

† Electronic address: s.miret@imaff.cfmac.csic.es

- [1] D.A. Micha and I. Burghardt (eds.), *Quantum Dynamics of Complex Molecular Systems* (Springer, Berlin, 2006).
- [2] W. Pauli, *Die allgemeine Prinzipien der Wellenmechanik*, in *Handbuch der Physik*, H. Geiger and K. Scheel (eds.) (Springer-Verlag, Berlin, 1933), Vol. 24, part 1, 2nd ed.
- [3] R.A. Leacock, M.J. Padgett, *Phys. Rev. Lett.* **50**, 3 (1983); *Phys. Rev. D* **28**, 2491 (1983).
- [4] M.V. John, *Found. Phys. Lett.* **15**, 329 (2002).
- [5] A.S. Sanz, F. Borondo, and S. Miret-Artés, *J. Phys.: Condens. Matter* **14**, 6109 (2002); R. Guantes, A.S. Sanz, J. Margalef-Roig, and S. Miret-Artés, *Surf. Sci. Rep.* **53**, 199 (2004).
- [6] C.-C. Chou and R.E. Wyatt, *Phys. Rev. E* **74**, 066702 (2006); *J. Chem. Phys.* **125**, 174103 (2006); *Phys. Rev. A* **76**, 012115 (2007).
- [7] Y. Goldfarb, I. Degani, and D. Tannor, *J. Chem. Phys.* **125**, 231103 (2006); *J. Chem. Phys. (Reply)* (in press, 2007); Y. Goldfarb, J. Schiff, and D.J. Tannor, *J. Chem. Phys.* (in press, 2007).
- [8] A.S. Sanz and S. Miret-Artés, *J. Chem. Phys.* (in press, 2007).
- [9] C.-D. Yang, *Ann. Phys. (N.Y.)* **319**, 399 (2005); *Ann. Phys. (N.Y.)* **319**, 444 (2005); *Chaos, Solit. and Fract.* **30**, 342 (2006).
- [10] J. Barker-Jarvis and P. Kabos, *Phys. Rev. A* **68**, 042110 (2003).
- [11] A.S. Sanz, F. Borondo, and S. Miret-Artés, *Phys. Rev. B* **69**, 115413 (2004); *J. Chem. Phys.* **120**, 8794 (2004).
- [12] A.S. Sanz and S. Miret-Artés (to be submitted, 2007).
- [13] A.S. Sanz and S. Miret-Artés (to be submitted, 2007).
- [14] A. S. Sanz and S. Miret-Artés, *J. Chem. Phys.* **126**, 234106 (2007).